Electronic Supplementary Information

SiO_2-protected shell mediated templating synthesis of Fe-N-doped carbon nanofibers and their enhanced oxygen reduction reaction performance

Bi-Cheng Hu‡, Zhen-Yu Wu‡, Sheng-Qi Chu, Hong-Wu Zhu, Hai-Wei Liang, Jing Zhang, and Shu-Hong Yu**

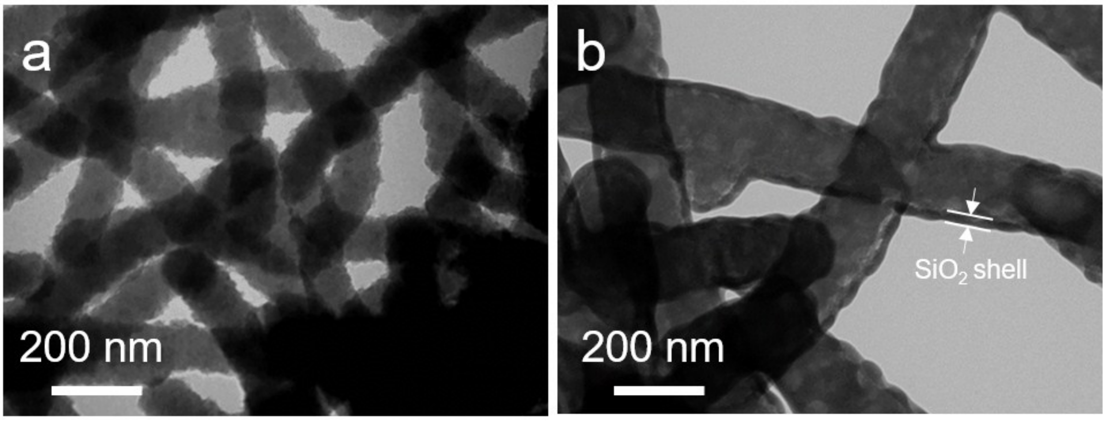

Fig. S1. TEM images of (a) CNF@PPy and (b) CNF@PPy@SiO_2. The layer of SiO_2 coating on CNFs can be clearly observed from the TEM image in (b).

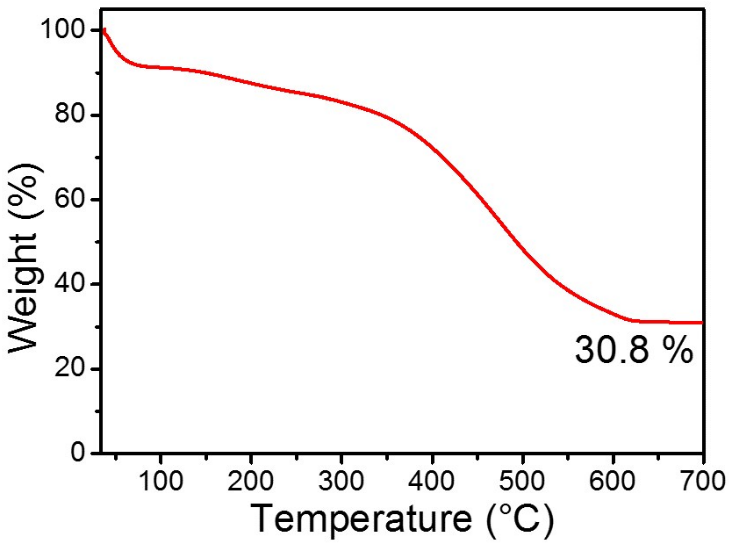

Fig. S2. TGA curves of CNF@PPy@SiO_2 in air.

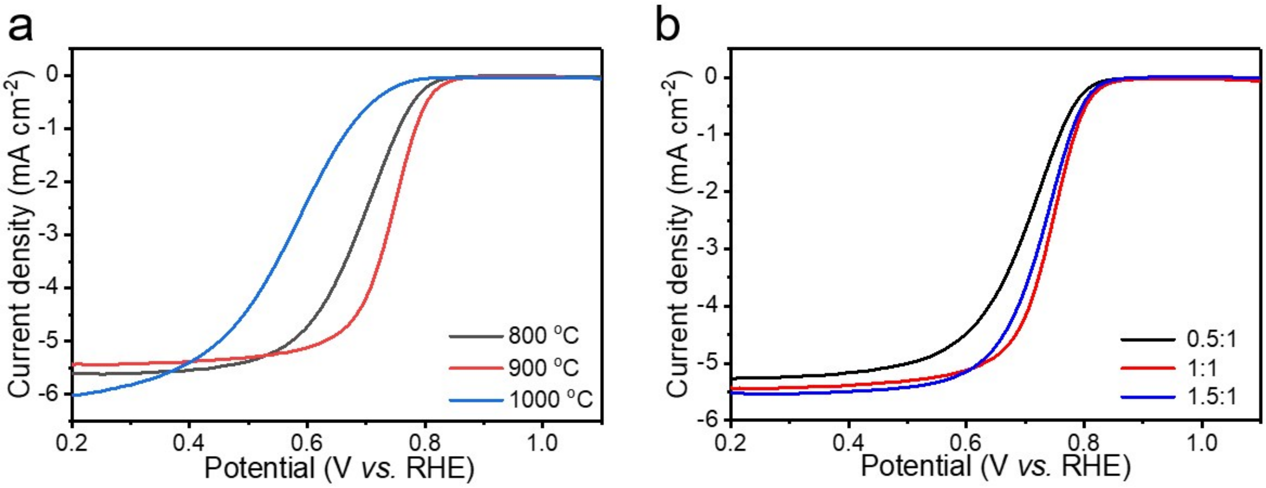

Fig. S3. LSV curves of p-Fe-N-CNFs catalysts prepared under a) different pyrolysis temperatures, b) different $FeCl_3$ adding amounts.

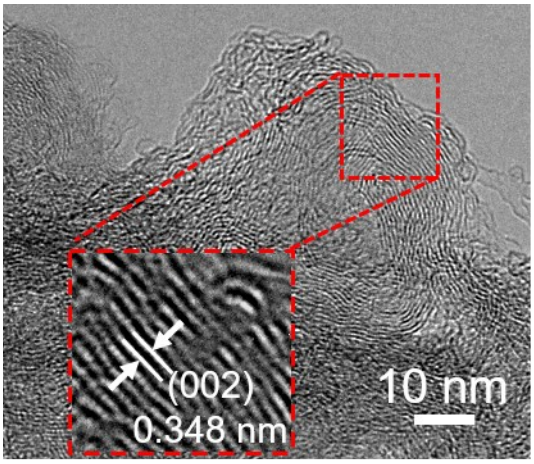

Fig. S4. HRTEM images of p-Fe-N-CNFs. The inset is an enlarged HRTEM image.

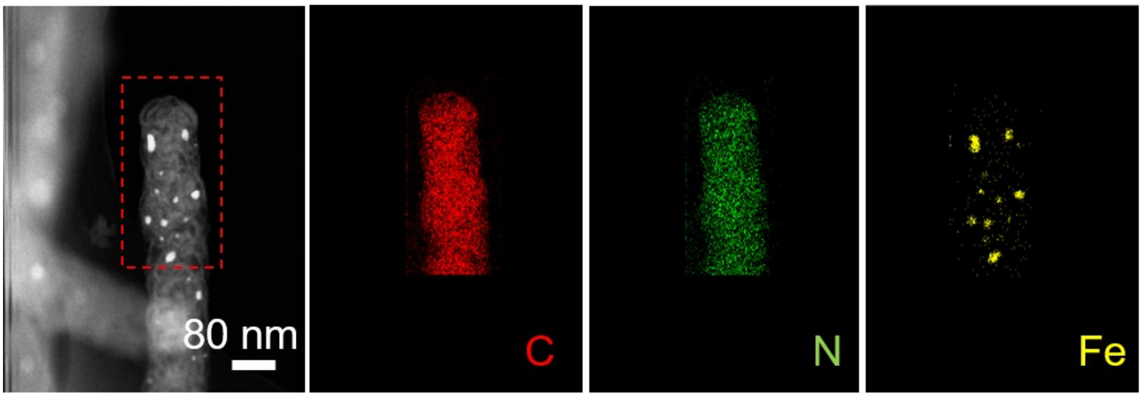

Fig. S5. Elemental mapping of the up-Fe-N-CNFs catalyst.

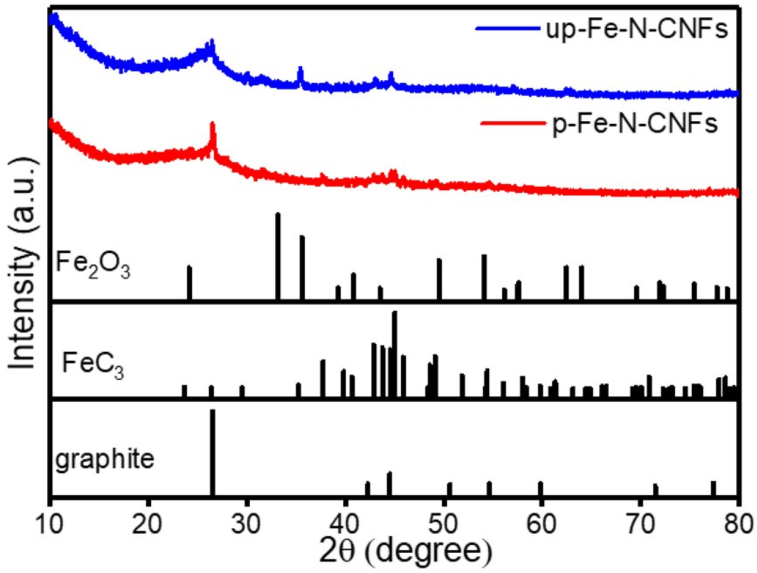

Fig. S6. XRD pattern of p-Fe-N-CNFs and up-Fe-N-CNFs.

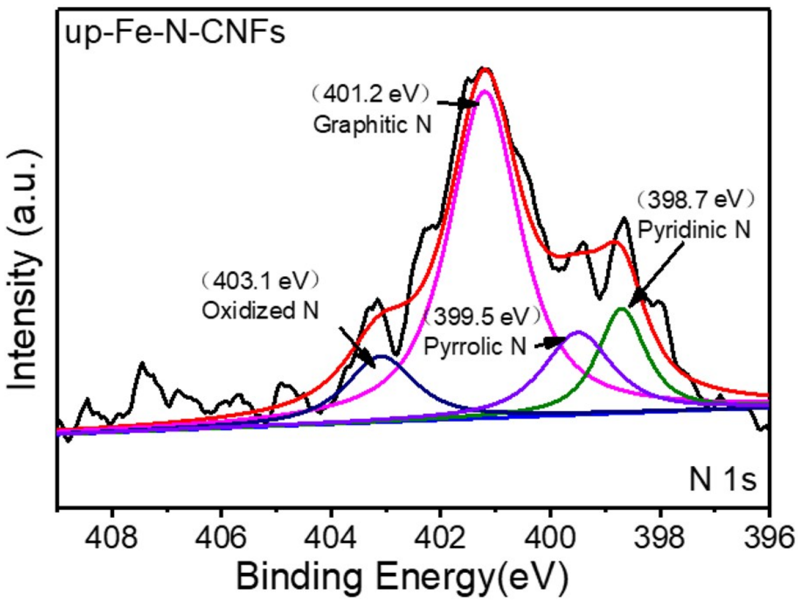

Fig. S7. High-resolution N 1s spectra of up-Fe-N-CNFs.

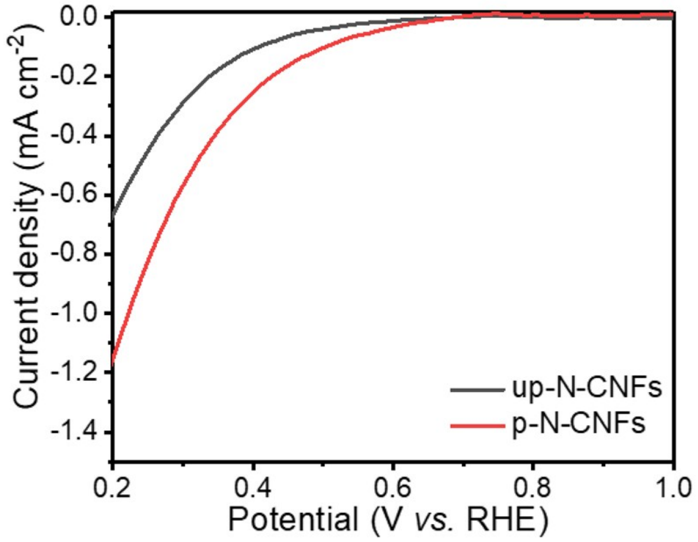

Fig. S8. LSV curves of up-N-CNFs and p-N-CNFs.

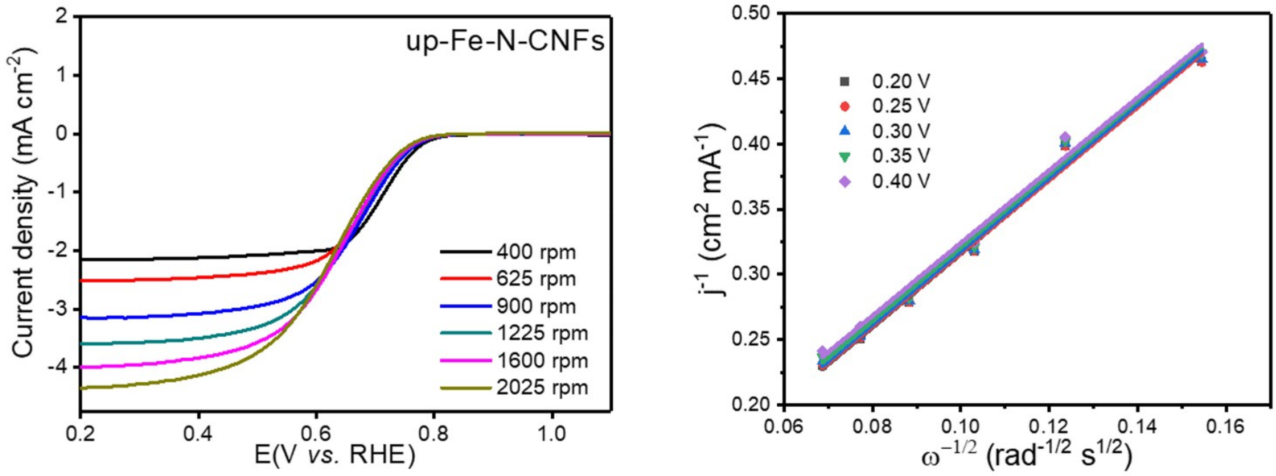

Fig. S9. LSV curves with various rotation rates (a) and corresponding K-L plots (j^{-1} vs. $\omega^{-1/2}$) (b) at different potentials of up-Fe-N-CNFs.

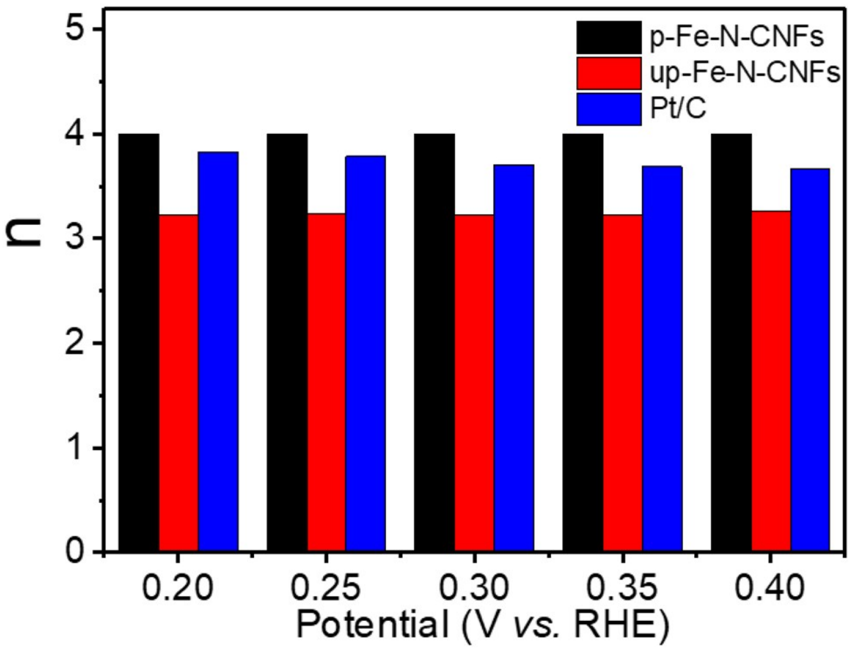

Fig. S10. Electron transfer number (n) of p-Fe-N-CNFs, up-Fe-N-CNFs and Pt/C catalysts under various potentials.

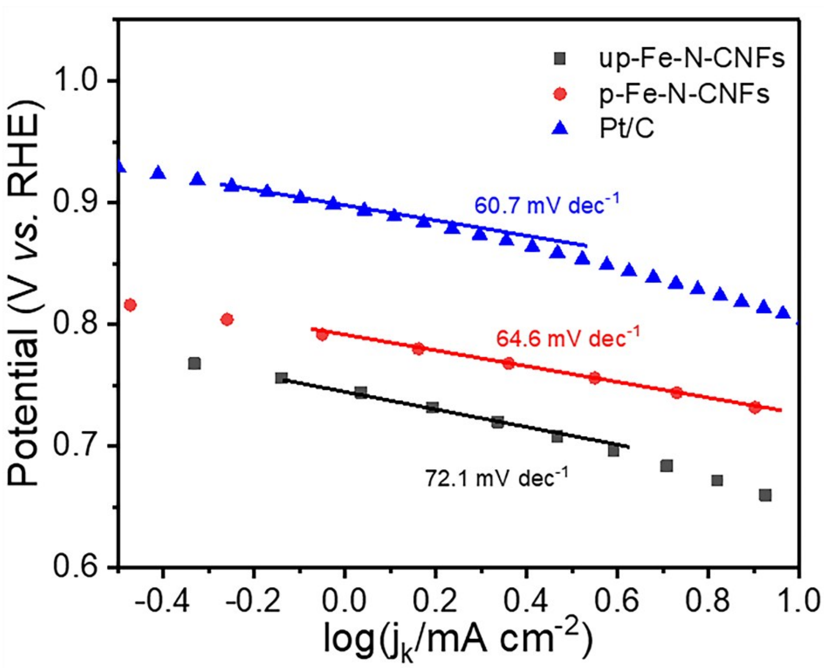

Fig. S11. Tafel plots of p-Fe-N-CNFs, up-Fe-N-CNFs, and Pt/C catalysts.

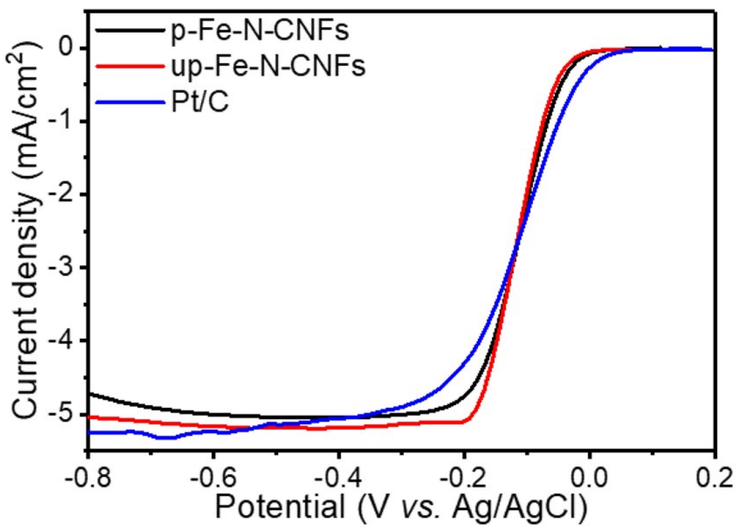

Fig. S12. LSV curves of p-Fe-N-CNFs, up-Fe-N-CNFs, and 20% Pt/C in 0.1 M KOH solution.

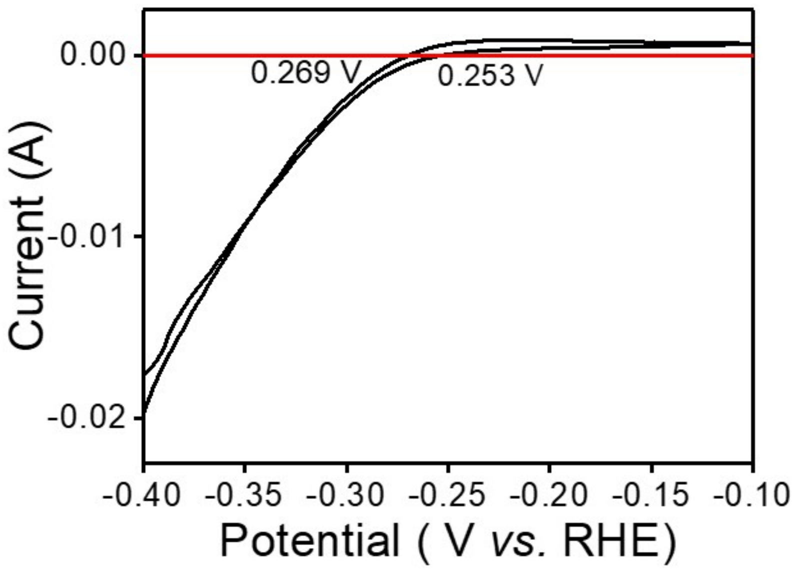

Fig. S13. The CV result of RHE calibration in 0.1 M $HClO_4$ solution, Potential (V *vs.* RHE) = Potential (V *vs.* Ag/AgCl) + 0.261 V.

Table S1. The nitrogen and iron content of p-Fe-N-CNFs prepared at different temperature (800-1000 ^{o}C) obtained by XPS.

samples	N (at%)	Fe (at%)
p-Fe-N-CNFs-800	8.80	0.22
p-Fe-N-CNFs-900	6.23	0.31
p-Fe-N-CNFs-1000	3.03	0.12

Table S2. Pore features of p-Fe-N-CNFs and up-Fe-N-CNFs, respectively.

Catalyst	S_{BET}* (m^2 g^{-1})	S_{micro}† (m^2 g^{-1})	S_{micro}/S_{meso}‡	V_t§ (m^3 g^{-1})	V_{micro}‖ (m^3 g^{-1})	V_{micro}/V_{meso}¶
p-Fe-N-CNFs	941.015	664.102	2.40	0.7829	0.3519	0.82
up-Fe-N-CNFs	652.976	217.458	0.50	0.7005	0.2257	0.47

*S_{BET} is the Brunauer-Emmett-Teller (BET) specific surface area.
†S_{micro} is the t-plot-specific micropore surface area calculated from the N_2 adsorption-desorption isotherm.
‡S_{meso} is the specific mesopore surface area estimated by subtracting S_{micro} from S_{BET}.
§V_t is the total specific pore volume determined by using the adsorption branch of the N_2 isotherm at P/P_0=0.99.
‖V_{meso} is the specific mesopore volume obtained from the Barrett-Joyner-Halenda (BJH) cumulative specific adsorption volume of pores of 3.00-300.00 nm in diameter.
¶V_{micro} is the specific micropore volume calculated by subtracting V_{meso} from V_t.

Table S3. Comparison of ORR performance in acidic electrolyte of p-Fe-N-CNFs at 1600 rpm with literature values.

Catalyst	Onset potential (V vs. RHE)	Half-wave potential (V vs. RHE)	Current density at 0.3 V (mA cm^{-2})	Electrolyte	References
Fe-N/C-800	0.77	~0.6	4.88	0.1 M $HClO_4$	J. Am. Chem. Soc. 2015,137, 5555
CPANI-Fe- NaCl	/	~0.727	~5	0.1 M $HClO_4$	J. Am. Chem. Soc. 2015, 137, 5414
PmPDA-FeNx/C	~0.94 (900 rpm)	0.82 (900 rpm)	/	0.1 M H_2SO_4	J. Am. Chem. Soc. 2014, 136, 10882
PMF-800	/	~0.62	~6	0.1 M $HClO_4$	J. Am. Chem. Soc. 2015, 137, 1436
FePhen@MOF-$ArNH_3$	0.93	0.77	~5.9	0.1 M $HClO_4$	Nat. Commun. 2015, 6, 7343
PANI-Fe/SiO_2 colloid	0.84	0.73	~4.6	0.5 M H_2SO_4	J. Am. Chem. Soc. 2013, 135, 16002
Fe/N/C-SCN	/	0.836 (900 rpm)	/	0.1 M H_2SO_4	Angew. Chem. Int. Ed. 2015, 54 ,9907
Fe_3C/C-700	0.9	0.73	~4.2	0.1 M $HClO_4$	Angew. Chem. Int. Ed. 2015, 53, 3675
Fe-CNT-PA	/	~0.41	~5.78	0.5 M H_2SO_4	Energy Environ. Sci., 2015, 8, 1799
Fe_3C/NG-800	0.92	0.77	~5.8	0.1 M $HClO_4$	Adv. Mater. 2015, 27, 2521
(Fe,Co)/N-C	1.06	0.863	~5.5	0.1 M $HClO_4$	J. Am. Chem. Soc., 2017, 139, 17281-17284
Fe-ZIF	/	0.85 (900 rpm)	/	0.5 M H_2SO_4	J. Am. Chem. Soc., 2017, 139, 14143-14149
Fe/SNC	/	0.77	4.8	0.5 M H_2SO_4	Angew.Chem. Int. Ed. 2017, 56,13800-13804
FeTMPPCl	0.824	0.748	~6	0.1 M $HClO_4$	Adv. Funct. Mater. 2017, 1604356
up-Fe-N-CNFs	**0.81**	**0.68**	**5.0**	**0.1 M $HClO_4$**	**This work**
p-Fe-N-CNFs	**0.85**	**0.74**	**5.5**	**0.1 M $HClO_4$**	**This work**

Table S4. Comparison of ORR performance of p-Fe-N-CNFs at 1600 rpm in 0.1 M KOH with literature values.

Catalyst	Onset potential (V vs. RHE)	Half-wave potential (V vs. RHE)	Current density at 0.4 V (mA cm^{-2})	References
Fe-N/C-800	0.98	~0.81	4.81	J. Am. Chem. Soc. 2015, 137, 5555
Fe_3C/C-800	1.05	0.83	/	Angew. Chem. Int. Ed. 2014, 53, 3675
Fe-N/C	0.923	0.809	~6.0	J. Am. Chem. Soc. 2014, 136, 11027
FePhen@MOF-$ArNH_3$	1.03	0.86	~5.1	Nat. Commun. 2015, 6, 7343
Fe-tpy-GO	<-0.10 (*vs.* Ag/AgCl)	<-0.40 (*vs.* Ag/AgCl)	-3.5	Angew. Chem. Int. Ed. 2014, 53, 1415
PMF-800	/	~0.86	~5.7	J. Am. Chem. Soc. 2015, 137, 1436
Fe_3C/NG-800	1.03	0.86	~5.7	Adv. Mater. 2015, 27, 2521
Fe@C-FeNC-2	/	0.899	~5.3	J. Am. Chem. Soc. 2016, 138, 3570
Fe_3O_4/N-GAs	−0.19 (*vs.* Ag/AgCl)	<-0.40 (*vs.* Ag/AgCl)	-3.3	J. Am. Chem. Soc. 2012, 134, 9082
Fe-NMCSs	1.027	0.86	~5.2	Adv. Mater. 2016, 28, 7948
FP-Fe-TA-N-850	0.98	/	5.0 (0.6 V)	Angew. Chem. Int. Ed. 2015, 55, 1355
Fe-N-CNFs	0.93	0.81	5.12	Angew. Chem. Int. Ed. 2015, 54 ,8179
NC@Co-NGC DSNCs	0.92	0.82	5.3	Adv. Mater. 2017, 1700874
pCNT@Fe@GL/CNF	/	0.811	5.7	Adv. Mater. 2017, 1606534
p-Fe-N-CNFs	**0.94**	**0.82**	**5.05**	**This work**